



**HAL**  
open science

# Emergence of Supercoiling-Mediated Regulatory Networks through Bacterial Chromosome Organization

Théotime Grohens, Sam Meyer, Guillaume Beslon

► **To cite this version:**

Théotime Grohens, Sam Meyer, Guillaume Beslon. Emergence of Supercoiling-Mediated Regulatory Networks through Bacterial Chromosome Organization. 2024. hal-04398893

**HAL Id: hal-04398893**

**<https://hal.science/hal-04398893>**

Preprint submitted on 18 Jan 2024

**HAL** is a multi-disciplinary open access archive for the deposit and dissemination of scientific research documents, whether they are published or not. The documents may come from teaching and research institutions in France or abroad, or from public or private research centers.

L'archive ouverte pluridisciplinaire **HAL**, est destinée au dépôt et à la diffusion de documents scientifiques de niveau recherche, publiés ou non, émanant des établissements d'enseignement et de recherche français ou étrangers, des laboratoires publics ou privés.



Distributed under a Creative Commons Attribution 4.0 International License

# Emergence of Supercoiling-Mediated Regulatory Networks through Bacterial Chromosome Organization

Théotime Grohens<sup>1</sup>      Sam Meyer<sup>2</sup>  
Guillaume Beslon<sup>3,\*</sup>

<sup>1</sup>Centre for Genomic Regulation, Barcelona Institute of Science and Technology,  
Dr. Aiguader 88, Barcelona 08003, Spain

<sup>2</sup>Université de Lyon, INSA Lyon, Université Claude Bernard Lyon 1, CNRS,  
UMR5240 MAP, F-69622, France

<sup>3</sup>Université de Lyon, INSA Lyon, Inria, ECL, Université Claude Bernard Lyon 1,  
Université Lumière Lyon 2, CNRS, LIRIS UMR 5205, F-69622, France

\*Corresponding author: [guillaume.beslon@inria.fr](mailto:guillaume.beslon@inria.fr)

5

## Abstract

DNA supercoiling – the level of twisting and writhing of the DNA molecule around itself – plays a major role in the regulation of gene expression in bacteria by modulating promoter activity. The level of DNA supercoiling is a dynamic property of the chromosome, which varies both at the global scale in response to external factors such as environmental perturbations, and at the local scale in response to internal factors including gene transcription itself. These local variations can couple the transcription rates of neighboring genes by creating feedback loops. The importance of the role of such supercoiling-mediated interactions in the regulation of gene expression however remains uncertain. In this work, we study how this coupling could play a part in the bacterial regulatory landscape by coevolving with genome organization. We present a model of gene transcription and DNA supercoiling at the whole-genome scale, in which individuals must evolve gene expression levels adapted to two different environments. In this model, we observe the evolution of whole-genome regulatory networks that provide fine control over gene

10

15

expression by leveraging the transcription-supercoiling coupling, and show that the structure of these networks is underpinned by the organization of genes along the chromosome at several scales.

20 Local variations in DNA supercoiling could therefore jointly help shape both gene regulation and genome organization during evolution.

## 1 Introduction

DNA is the material basis of genetic information. It is a flexible polymer that comprises two strands of nucleotides that coil around each other, at a rate of 10.5 base pairs per turn in the absence of external  
25 constraints. When subjected to torsional stress, DNA can either writhe and form 3-dimensional loops, or twist around itself more or less tightly than in its relaxed state (Travers and Muskhelishvili, 2005). Both writhing and twisting are referred to as DNA supercoiling, and its level is measured as the relative density  $\sigma$  of supercoils in overwound (positively supercoiled,  $\sigma > 0$ ) or underwound (negatively supercoiled,  $\sigma < 0$ ) DNA compared to its relaxed state. In bacteria, DNA is normally maintained  
30 in a moderately negatively supercoiled state, with a reference value of  $\sigma_{basal} = -0.06$  in *Escherichia coli* (Travers and Muskhelishvili, 2005). In these organisms, DNA supercoiling is an important regulator of gene expression, as changes in the level of supercoiling directly affect gene transcription rates (Dorman and Dorman, 2016). But gene transcription in turn also affects DNA supercoiling (Liu and Wang, 1987; Visser et al., 2022), resulting in a coupling between transcription and supercoiling  
35 that has been termed the *transcription-supercoiling coupling* (Meyer and Beslon, 2014). This coupling has been suggested to play an important role in bacterial gene regulation, as it could allow for the presence of gene regulatory networks that do not depend on transcription factors, but could be directly rooted in the organization of the genome. In this manuscript, we question this hypothesis by using an *in silico* experimental evolution approach, in which we model the evolution of a population  
40 of organisms for which DNA supercoiling is the only regulator of gene expression.

**Regulation of DNA Supercoiling** In bacteria, the level of DNA supercoiling is primarily controlled by topoisomerases, enzymes that alter DNA supercoiling by cutting and rotating the DNA strands. The two main topoisomerases are gyrase, which dissipates positive supercoiling by introducing negative supercoils at an ATP-dependent rate, and topoisomerase I, which oppositely relaxes  
45 negative supercoiling (Champoux, 2001). However, numerous other processes also impact the level of DNA supercoiling, either by generating new supercoils or by constraining their diffusion. In particular,

according to the *twin-domain* model of supercoiling presented in Liu and Wang (1987), the transcription of a gene by an RNA polymerase generates both positive supercoils downstream and negative supercoils upstream of the transcriptional complex (Guo et al., 2021; Sutormin et al., 2022; Visser et al., 2022), as a consequence of the drag that hampers the rotation of the polymerase around DNA during transcription. Moreover, while the intrinsic flexibility of the DNA polymer would in principle allow supercoils to propagate freely along the chromosome, many nucleoid-associated proteins such as FIS, H-NS or HU bind to bacterial DNA (Krogh et al., 2018). These DNA-bound proteins together create barriers that block the diffusion of supercoils, resulting in what have been named *topological domains* of DNA supercoiling (Postow et al., 2004). The level of DNA supercoiling can additionally be affected by numerous environmental factors. Salt shock transiently increases negative DNA supercoiling in *E. coli* (Hsieh et al., 1991); an acidic intracellular environment relaxes DNA in the facultative pathogen *Salmonella enterica* var. Typhimurium (Marshall et al., 2000); and higher temperatures relax DNA in the plant pathogen *Dickeya dadantii* (H erault et al., 2014). These constraints overall paint the picture of a very dynamic *DNA supercoiling landscape* in bacteria (Visser et al., 2022), in which the supercoiling level varies in both time and space, during the bacterial lifecycle and along the bacterial chromosome.

**Global Regulatory Role of DNA Supercoiling** The level of DNA supercoiling influences gene expression, as more negatively supercoiled DNA facilitates the initiation of gene transcription. Opening the DNA double strand – the initial step of gene transcription – is thermodynamically favored in more negatively supercoiled DNA regions, and gene expression has indeed been shown to increase sigmoidally with the level of negative DNA supercoiling (El Houdaigui et al., 2019). Through this mechanism, DNA supercoiling has experimentally been shown to act as a broad regulator of gene expression in several model bacteria. In *E. coli*, Peter et al. (2004) showed that 7% of genes were sensitive to a global relaxation (a less negative supercoiling level) of chromosomal DNA, of which one third were up-regulated by relaxation and two thirds down-regulated. Similar results were obtained for *S. enterica*, in which 10% of genes were sensitive to DNA relaxation (Webber et al., 2013), and for *S. pneumoniae*, in which around 13% of genes were sensitive to relaxation (Ferrandiz et al., 2010). When oppositely inducing hypercoiling (more negative supercoiling) in *D. dadantii*, 13% of genes were affected in the exponential phase, and 7% of genes in the stationary phase (Pineau et al., 2022). In this bacteria, different genomic regions moreover exhibit markedly different responses to changes in the supercoiling level (Muskhelishvili et al., 2019), allowing for the expression of pathogenic genes in

stressful environments only.

Such a regulatory role of DNA supercoiling might be especially important in bacteria with reduced genomes, such as the obligate aphid endosymbiotic bacterium *B. aphidicola*. As *B. aphidicola* is nearly devoid of transcription factors, global and local changes in supercoiling are thought to be one of the main mechanisms for the regulation of gene expression available to this bacteria (Brinza et al., 2013). Finally, mutations that alter DNA supercoiling have also been shown to be evolutionarily favorable in experimental settings. For example, in the so-called *Long-Term Evolution Experiment*, 12 populations of *E. coli* cells seeded from a common ancestor have been adapting to a laboratory environment for over 75,000 generations (Lenski et al., 1991; Lenski, 2023). In this experiment, 10 out of the 12 populations were shown to present a higher level of negative supercoiling relative to their ancestor, with one population in particular presenting an increase of more than 17% in negative supercoiling (Croizat et al., 2005). In this population, a mutation in the *topA* gene (which encodes topoisomerase I) and a mutation in the *fis* gene (which encodes a histone-like protein) were both shown to increase negative supercoiling by 12% and 5% respectively when inserted back into the ancestral strain, and to provide a significant growth advantage (that is, higher fitness) relative to the ancestral strain. This evolutionary trajectory was then shown to be repeatable not only at the phenotypic level, but also at the genetic level, with 10 of the 12 strains harboring mutations in DNA supercoiling-related genes (Croizat et al., 2010). In the context of the *LTEE*, supercoiling mutations therefore played a role in the adaptation of *E. coli* strains to new environments, evidencing the important effect of DNA supercoiling on bacterial gene regulation.

**The Transcription-Supercoiling Coupling** The transcription of a given gene by an RNA polymerase generates an accumulation of positive and negative supercoiling on either side of the transcribed gene (Guo et al., 2021; Sutormin et al., 2022). Whenever a second gene is located closely enough to this first gene on the genome, the change in supercoiling at the location of the promoter of that second gene can impact its transcription rate, as more negative supercoiling facilitates gene transcription (Forquet et al., 2021). In turn, the transcription of that second gene can also generate a local change in supercoiling around the first gene, resulting in an interaction between the transcription levels of these two genes, which has been called the transcription-supercoiling coupling (Meyer and Beslon, 2014). Depending on the relative orientation of these genes, the coupling can take several forms. Divergent genes can increase their respective transcription level in a positive feedback loop; convergent genes can inhibit the transcription of one another; and in tandem genes, the transcription of the downstream

gene can increase the transcription of the upstream gene, while the transcription of the upstream gene  
110 can decrease the transcription of the downstream gene.

This supercoiling-mediated interaction between neighboring genes has been experimentally documented in several bacterial genetic systems. In the *E. coli*-related pathogen *Shigella flexneri*, the *virB* promoter is normally only active at high temperatures, but can be activated at low temperatures by the insertion of a phage promoter in divergent orientation (Tobe et al., 1995). Similarly, the expression of the *leu-500* promoter in *S. enterica* can be increased or decreased by the insertion of upstream  
115 transcriptionally active promoters, depending on their orientation relative to *leu-500* (El Hanafi and Bossi, 2000). Finally, the magnitude of the effect of the transcription-supercoiling coupling has also been explored in a synthetic construct in which the inducible *ilvY* and *ilvC* *E. coli* promoters were inserted on a plasmid in divergent orientations (Rhee et al., 1999). In this system, a decrease in the  
120 activity of *ilvY* has been associated with a decrease in *ilvC* activity, and an increase in *ilvY* activity with a corresponding increase in *ilvC* activity.

The biological relevance of the transcription-supercoiling coupling might however not be limited to these particular instances. Indeed, in *E. coli*, the typical size of topological domains – inside which the positive and negative supercoils generated by gene transcription can propagate – is usually estimated  
125 to range around 10 kb (Postow et al., 2004), and transcription-generated supercoiling has been shown to propagate up to 25 kb in each direction around some specific genes (Visser et al., 2022). As genes stand on average 1 kb apart on the *E. coli* chromosome (Blattner, 1997), any single topological domain could therefore encompass multiple genes that can interact via the transcription-supercoiling coupling. Supercoiling-sensitive genes have indeed been shown to group in up- or down-regulated clusters in bacteria such as *E. coli* (Peter et al., 2004), *S. enterica* (Webber et al., 2013) and *S. pneumoniae* (Ferrandiz et al., 2010). Focusing on *E. coli*, a statistical analysis of the relative position of neighboring genes on the chromosome of this bacteria indeed has shown that genes that are up-regulated by negative supercoiling have more neighbors in divergent orientations, while genes that are down-regulated by negative supercoiling have more neighbors in converging orientations (Sobetzko, 2016).  
135 The co-localization of genes in such clusters has therefore been hypothesized to play a phenotypic role by enabling a common regulation of their transcription through local variations in the supercoiling level. Finally, synteny segments – clusters of neighboring genes that show correlated expression patterns – have been shown to be conserved between *E. coli* and the distantly related *Bacillus subtilis* (Junier and Rivoire, 2016), possibly as a consequence of co-regulation of the genes within these segments through

140 supercoiling. Overall, this body of empirical evidence suggests that local variations in the supercoiling level, due to its coupling with transcription, could indeed play a substantial role in the regulation of gene activity and consequently impact the evolution of genome organization.

In this paper, we address the question of the effect of the transcription-supercoiling coupling in the evolution of the local and global organization of bacterial genomes, by studying its role as a regula-  
145 tory mechanism. To this end, we present a two-level individual-based artificial evolution framework, in which a whole-genome model of the transcriptional response of genes to the local transcription-generated level of supercoiling is embedded within an evolutionary simulation. In this framework, individuals must evolve gene expression levels that are adapted to two different environments, characterized by supercoiling level constraints, through chromosomal rearrangements only. We first show that  
150 complex environment-driven patterns of gene expression are present in evolved populations. In particular, we observe the emergence of a class of relaxation-activated genes, as have been observed in many real-world bacterial genomes. We furthermore characterize the spatial organization of genes along the genome that is responsible for these expression patterns. We show that genes are locally organized in convergent or divergent pairs of genes which leverage the transcription-supercoiling coupling for either  
155 mutual activation or inhibition. Then, we show that this local organization is not entirely sufficient to fully account for the complex gene expression patterns that we observe, but that obtaining gene inhibition in particular requires the coordination of a larger number of genes. Finally, we show that, in our model, genes form a densely connected genome-wide regulatory network, overall showing that supercoiling-based regulation could indeed coevolve with genome organization in bacterial genomes.

## 160 2 Results

### 2.1 Evolution of Gene Regulation through the Transcription-Supercoiling Coupling

We introduce a model (detailed in Methods) in which populations of individuals are described by their circular genome and whose gene expression levels depend on the local level of DNA supercoiling.  
165 Individuals in the model must adapt to two different environments, each characterized by their impact  $\delta\sigma_{env}$  on the background supercoiling level of individual genomes, by adjusting the expression levels of their genes. The first environment, named environment A, induces a global relaxation of DNA

which decreases baseline gene expression ( $\delta\sigma_{env} = \delta\sigma_A = 0.01$ ), as in the acidic macrophage vacuoles encountered by *S. enterica* (Marshall et al., 2000). The second environment, named environment B, 170 oppositely induces a global hypercoiling of DNA which increases baseline gene expression ( $\delta\sigma_{env} = \delta\sigma_B = -0.01$ ), as observed for example when shifting *E. coli* cultures to a salt-rich medium (Hsieh et al., 1991). In order to have a high fitness value in our model, an individual must display environment-specific gene expression patterns, obtained by the activation or inhibition of three disjoint subsets of its genes – called *A*, *B* and *AB* – in each environment. More precisely, *A* genes must be activated in 175 environment A but not in environment B, *B* genes in environment B but not in environment A, and *AB* genes must be activated in both environments. We define the expression level of the genes of a given individual in each of these environments as the solution to the system of equations that are given by the supercoiling-mediated interactions between the transcription of neighboring genes (Equations 1 to 4 in Methods). At every generation of the simulation, we compute the fitness of every individual 180 based on these gene expression levels, then create the next generation by making individuals reproduce proportionally to their fitness, and applying random mutations to their offspring. Importantly, in order to focus on the evolution of genome organization, the only mutational operator that we use is genomic inversions, which can reorder genes on the genome and thereby affect gene expression levels and fitness.

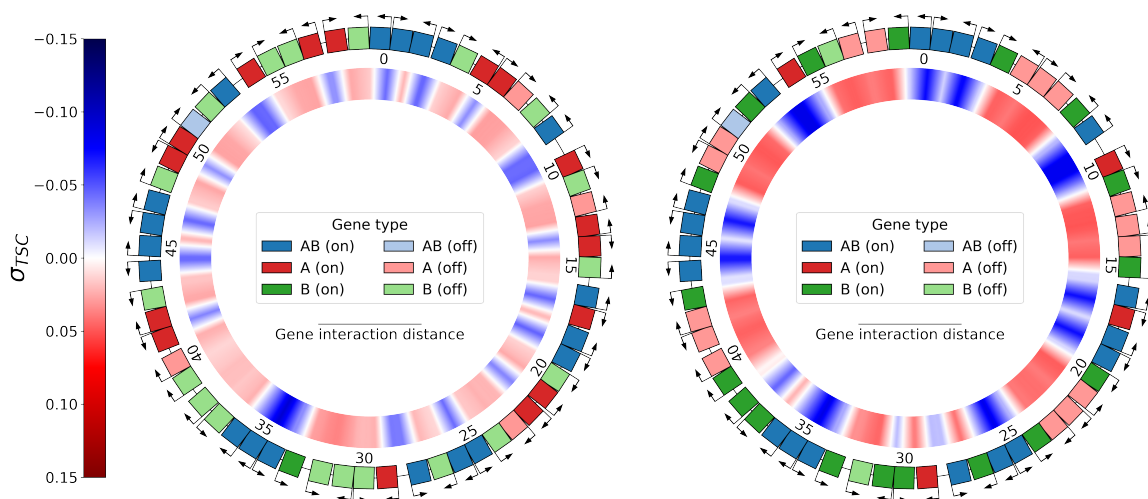


Figure 1: Genome of the best individual at the last generation of evolution of replicate 21, evaluated in the two environments: A (relaxed DNA, left) and B (hypercoiled DNA, right). The outer ring shows the type, orientation, and expression of each gene on the genome (darker color: activated; lighter color: inhibited). Genes are considered to be activated if their expression is above the threshold  $e_{1/2}$ , and inhibited otherwise (see Methods). Genes are numbered clockwise according to their position on the genome. The inner ring shows the level of transcription-generated DNA supercoiling  $\sigma_{TSC}$  at every position on the genome. Shades of blue represent negative supercoiling ( $\sigma_{TSC} < 0$ ), and shades of red positive supercoiling ( $\sigma_{TSC} > 0$ ).

**Evolution of Environment-Specific Gene Expression Levels** Using the model presented above, we let 30 populations of 100 individuals evolve for 1,000,000 generations. The genome of a typical individual at the end of the evolutionary simulation is depicted in Figure 1, in environments A (left) and B (right). The outer ring depicts gene position, orientation, type, and activation, and the inner ring the local level of supercoiling. We consider that a gene is activated if its expression is above the expression threshold  $e_{1/2}$ , and inhibited otherwise (see Methods). Different activation patterns are visible on the genome of this individual, for each gene type, as a function of the environment. All the *AB* genes except one (gene 51) are correctly activated (dark blue) in the two environments; 19 out of 20 *B* genes are correctly inhibited (light green) in environment A (left) while 18 are correctly activated (dark green) in environment B (right); and 16 *A* genes are activated (dark red) in environment A, while 16 are inhibited (light red) in environment B. Note that this asymmetry between the number of *A* and *B* genes that are in the expected state is due to an asymmetry in the effect of the environments themselves, which we will discuss below in more detail.

The transcription-generated supercoiling that is represented in the inner ring can also be seen to change consistently with the gene activation patterns between the two environments: zones of negative

DNA supercoiling (in blue) are delineated by divergently oriented activated genes, while zones of positive DNA supercoiling (in red) contain inhibited genes. The genome of this evolved individual therefore shows that, in the context of this model, it is possible for evolution to adjust gene expression levels to an environment-dependent target solely by rearranging relative gene positions and leveraging the transcription-supercoiling coupling between neighboring genes.

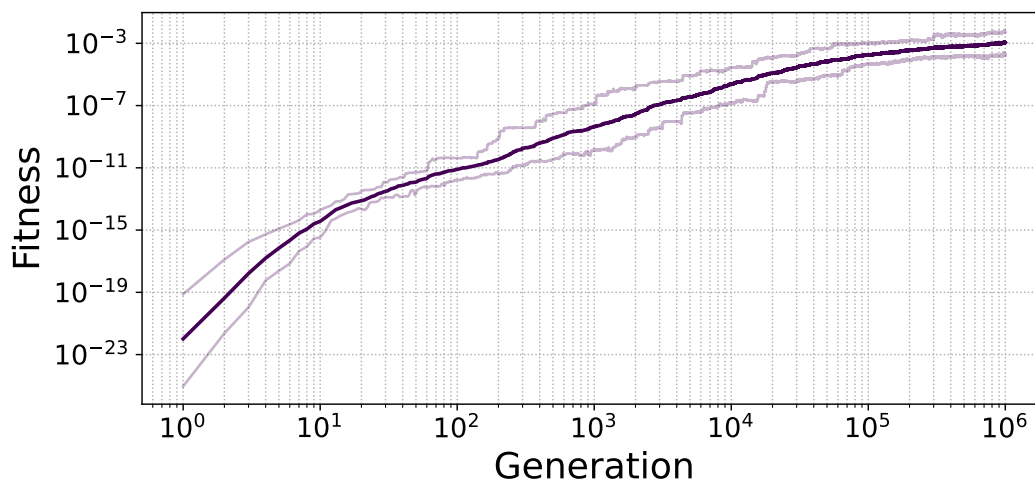


Figure 2: Geometric average of the fitness of the best individual in each of the 30 populations, at every generation. Lighter lines represent the first and last decile of the data.

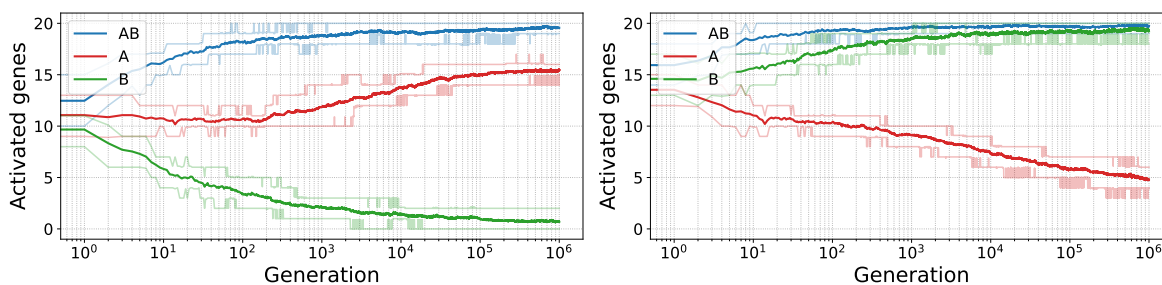


Figure 3: Average number of activated genes (expression higher than  $e_{1/2}$ ) of each type in the best individual at every generation, averaged over the 30 populations, in environments A (left) and B (right). Lighter lines represent the first and last decile of the data.

This behavior is however not specific to this particular individual. Figure 2 shows that the fitness of the best individual of each population, averaged over all the populations, evolves smoothly towards higher values over the course of the simulation. More precisely, Figure 3 shows that the numbers of activated genes of each particular type also evolve towards their respective targets, in environment A (left) and B (right). In each environment, the average number of activated *AB* genes (in blue) quickly

nearly reaches 20, its maximum value, as expected from their target; *B* genes (in green) follow the  
210 same behavior, evolving towards nearly full activation in environment B and nearly full inhibition in  
environment A. *A* genes (in red) follow a slightly different course, as the number of activated *A* genes  
seems to converge to approximately 15 out of the expected 20 in environment A, but continues to  
decrease towards the expected 0 in environment B by the end of the simulations.

The incomplete match of *A* genes with their evolutionary target – as compared to *B* genes – could  
215 however be partially expected. Environment A is indeed characterized by a *less negative* global super-  
coiling level, while environment B is characterized by a *more negative* global supercoiling level. As less  
negative supercoiling reduces gene transcription, it is by construction more difficult for a gene to have  
a high transcription rate in environment A than in environment B. *A* genes must therefore complete  
the more difficult task of being activated in the inhibiting environment A, while being inhibited in  
220 the activating environment B, whereas *B* genes must complete the comparatively easier task of being  
activated in the “easier” environment and inhibited in the “harder” environment.

Well-differentiated expression levels nonetheless evolve in our model for both types of genes, in  
response to the different supercoiling levels imposed by the environmental conditions. These patterns  
of gene expression are moreover remarkably robust to the difference between the environments. Indeed,  
225 we observe such patterns even when repeating the experiment with environmental perturbations 10  
and 100 times smaller in magnitude (see Supplementary Figures S1 and S2).

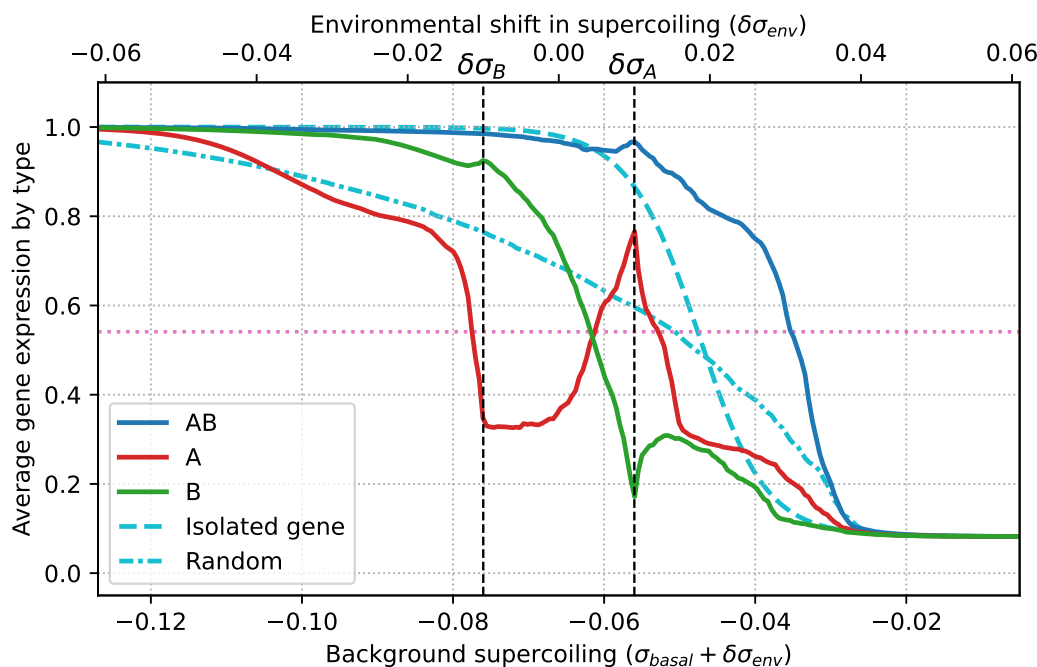


Figure 4: Average gene expression level for each type of gene ( $AB$ ,  $A$ , and  $B$  in blue, red, and green respectively), as a function of the background supercoiling level  $\sigma_{basal} + \delta\sigma_{env}$  (see Methods), averaged over every gene of that type in the best individual of each of the 30 replicates. The dashed vertical lines represent the supercoiling effect  $\delta\sigma_A$  and  $\delta\sigma_B$  of environments  $A$  and  $B$ , in which individuals evolve during the simulation, and the pink horizontal line marks  $e_{1/2}$ , the threshold above which a gene is considered active. The dashed light blue line represents the expression level of a single neighbor-less gene, and the dash-dotted light blue line represents the average expression level of genes on a random genome.

**Evolution of Relaxation-Activated Genes** In our model, the expression level of an isolated gene increases exponentially with the opening free energy of its promoter, which itself increases as a sigmoidal function of negative supercoiling (see Equations 3 and 4 in Methods). When measuring  
 230 the response of the genes of an evolved individual to a variation in the background supercoiling level (the sum of the basal supercoiling level  $\sigma_{basal}$  and of the environmental perturbation  $\delta\sigma_{env}$ ), one could naively expect a qualitatively similar response.

Figure 4 shows the average expression level of genes of each type as a function of the background supercoiling level, or equivalently as a function of the environmental perturbation (upper horizontal  
 235 axis), since the basal supercoiling level is kept constant in our model. It highlights striking differences between the responses of genes of each type in evolved genomes, when compared to isolated, non-interacting genes in our model (dashed light blue line) and to the average response of genes in random non-evolved genomes (dash-dotted light blue line). While  $AB$  and  $B$  genes (in blue and green

respectively) display an average expression level that decreases with the level of negative supercoiling, and that remains qualitatively similar to the behavior of random genes (dash-dotted line), *A* genes (in red) display a completely different behavior. Indeed, *A* genes show a non-monotonic response to environmental supercoiling, as their average expression level decreases until a local minimum in expression at  $\delta\sigma_B$ , then increases – even though background negative supercoiling decreases – until a local maximum at  $\delta\sigma_A$ , before decreasing again similarly to other genes types. In other words, due to their interaction with their neighbors, *A* genes present a phenotype of activation by environmental relaxation of DNA, for perturbations between  $\delta\sigma_B$  and  $\delta\sigma_A$ , even though the promoter activity of an isolated *A* gene decreases with background DNA relaxation (dashed light blue line). The evolution of this relaxation-activated phenotype is furthermore very robust, as we can observe it when replaying the main experiment with environments responsible for a 10 or 100 times smaller supercoiling perturbation than in the main experiment (see Supplementary Figures S3 and S4 respectively).

In our model, the transcription-supercoiling coupling is therefore able to provide a regulatory layer that mediates the transcriptional response to the global variation in DNA supercoiling caused by environmental perturbations. Indeed, it remarkably allows for the evolution of a transcriptional response to supercoiling that is opposite not only to that displayed by a non-interacting, neighborless gene, but also to that of randomly positioned genes, therefore demonstrating the importance of relative gene positions on transcriptional activity.

## 2.2 Evolution of Local Genome Organization

Having first characterized the different patterns of gene transcription that evolved in our simulations in response to different environmental conditions, we then sought to determine the genome organization that necessarily underlies these patterns in our model, given that the only difference between individuals in the model is the relative position and orientation of the genes on their genomes.

We started by studying genome organization at the most local level: pairs of neighboring genes. We measured the relative abundance of such pairs in each relative orientation (convergent, divergent, or tandem), as the relative orientation of two neighboring genes determines their mode of interaction through the transcription-supercoiling coupling: mutual activation for divergent genes, mutual inhibition for convergent genes, and activation (resp. inhibition) of the upstream (resp. downstream) gene by the downstream (resp. upstream) gene.

As, in our model, different gene types must evolve different activation patterns in each environment

for an individual to have high fitness, we additionally stratified these pair counts by the type of each  
 270 gene in the pair, resulting in 9 kinds of gene pairs. Finally, in order to quantify the actual strength  
 of the coupling between the genes in a given type of pair, we also summed the total level of positive  
 and negative supercoiling generated by the transcription of each gene in the pair at the promoter of  
 the other gene in the pair, for all relative orientations. These data are presented in Figure 5, with the  
 left-hand side panel showing the number of gene pairs of each kind, and the right-hand side panel the  
 275 corresponding transcription-generated supercoiling levels.

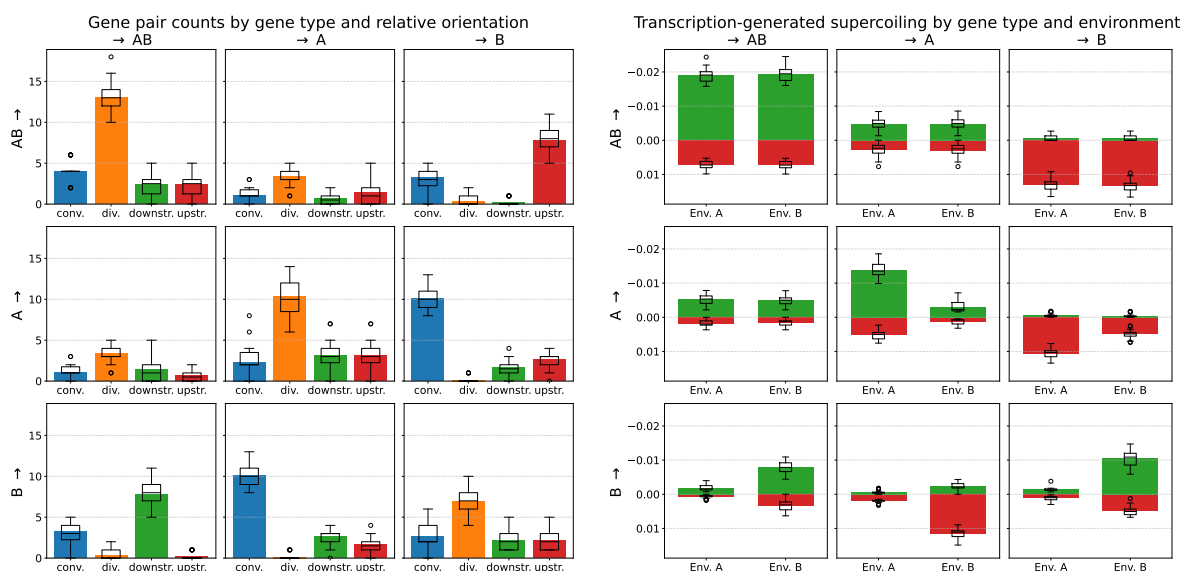


Figure 5: Interactions between pairs of neighboring genes. The left-hand side panel shows the number of gene pairs of each kind, split by the type of the focal gene (row) and of the second gene (column) in the pair, and by relative orientation (bars in each sub-panel: convergent, divergent, upstream, or downstream). For instance, the  $AB \rightarrow B$  top-right panel shows the influence of  $AB$  genes on  $B$  genes, and the  $B \rightarrow AB$  bottom-left panel the influence of  $B$  genes on  $AB$  genes (in the same pairs). In these pairs, there are on average 7.8  $AB$  genes directly upstream of a  $B$  gene (top-right panel, in red), or equivalently 7.8  $B$  genes directly downstream of an  $AB$  gene (bottom-left panel, in green) on an evolved genome. The right-hand side panel shows, for each kind of gene pair, the total amount of negative (green) and positive (red) transcription-generated supercoiling due to each gene type (row) measured at the promoter of each gene type (column), summed over all orientations, and split by environment. All data is averaged over the final best individual of each of the 30 replicates, and box plots indicate the median and the dispersion between replicates.

**Genomes Are Enriched in Divergent  $AB/AB$  Gene Pairs** The most frequent kind of gene  
 pair in evolved genomes is divergently oriented  $AB/AB$  pairs. 13 such pairs are found on each genome  
 on average ( $AB \rightarrow AB$  sub-panel on the left-hand side of Figure 5), out of a possible maximum of 20  
 (since any given gene can only be part of a single divergent pair), meaning that two-thirds of  $AB$  genes  
 280 are part of a divergent pair with another  $AB$  gene. These mostly divergent  $AB/AB$  gene pairs generate

an average negative supercoiling of around -0.012 at their promoters, in both environments (summing the positive and negative bars in the  $AB \rightarrow AB$  sub-panel on the right-hand side of Figure 5). This value is comparable in magnitude to – but has the opposite sign than – the shift in supercoiling that is caused by environment A ( $\delta\sigma_A = 0.01$ ). This shows that the interaction between neighboring genes  
285 can locally counteract the global shift in supercoiling caused by this environment, in order to maintain environment-agnostic high gene expression levels.

As shown in Figure 5, genomes also contain divergent  $A/A$  and  $B/B$  gene pairs, although less frequently than divergent  $AB/AB$  pairs. As both  $A$  genes and  $B$  genes must be conditionally expressed or inhibited depending on the environment, the unconditionally positive feedback loop resulting from a  
290 divergent orientation seems less evolutionarily favorable for  $A/A$  or  $B/B$  pairs than for  $AB/AB$  pairs. Consistently with this observation, divergent  $A/A$  and  $B/B$  pairs result in slightly weaker interactions (middle and bottom-right sub-panel of the right-hand side of Figure 5), in the environment in which these genes are active. On the contrary, divergent  $A/B$  gene pairs are almost never found, consistently with theoretical expectation, since  $A$  and  $B$  genes must not be expressed in the same environment.

**295 Genomes are Enriched in Convergent  $A/B$  Gene Pairs** The pattern in which  $B$  genes appear most frequently, and  $A$  genes nearly most frequently (just after divergent  $A/A$  pairs), is that of convergent  $A/B$  gene pairs. In this case, each gene in the pair theoretically inhibits the expression of the other gene. In environment A,  $A$  genes indeed generate an average positive supercoiling variation of 0.01 at the promoter of convergently oriented  $B$  genes, and hence decrease the expression of such  
300  $B$  genes with a strength that is comparable to the environmental change in supercoiling, similarly to  $AB/AB$  pairs above. In this environment,  $B$  genes are mostly inhibited, and therefore do not strongly impact the expression of  $A$  genes. In environment B, it is oppositely  $B$  genes that strongly inhibit the expression of convergently oriented  $A$  genes, through the generation of positive supercoiling at the promoter of such  $A$  genes. Convergently oriented  $A/B$  gene pairs therefore behave as toggle switches,  
305 or bistable gene regulatory circuits, in which the expression of one gene represses the expression of the other gene (Gardner et al., 2000).

In our model, the effect of the transcription-supercoiling coupling is therefore strong enough that specific local genome organizations can be evolutionarily selected for in order to attain favorable gene expression levels. In particular, we observe the formation of divergent pairs when consistently high  
310 expression is required, and of toggle switches when an environment-specific switch between activation and inhibition are required.

## 2.3 Pairwise Interactions Do Not Recapitulate the Regulatory Network

As we just saw, pairwise interactions between neighboring genes seem to play an important role in the regulatory response to environmental changes in supercoiling in our model. However, this local response cannot suffice to completely explain the environment- and gene-type- specific activation patterns that we observe; in particular,  $A/B$  toggle switches have to be pushed towards one stable state or the other by external factors. In the dense bacteria-like genomes of individuals in our model, genes indeed do not only interact with their closest neighbors, but also with genes located further away on the genome. In order to quantify more precisely the extent to which pairwise interactions can explain this regulatory response, we therefore studied the behavior of genes when considered as part of contiguous neighborhoods of increasing sizes.

For every odd subnetwork size  $k$  between 1 and the genome size, and for every gene on the genome, we extracted the subnetwork of  $k$  consecutive genes centered around that gene, computed the expression level of every gene in this subnetwork (in the same way as for a complete genome) in each environment, and compared the expression level of the central gene with its value in the complete genome. This allowed us to compute the minimum subnetwork size at which a gene presents the same activation state as in the complete genome, which we interpret as an indicator of the complexity of the interaction network required to produce the behavior of that particular gene. Two representative examples of this process are presented in Figure 6, and the complete results are shown in Figure 7.

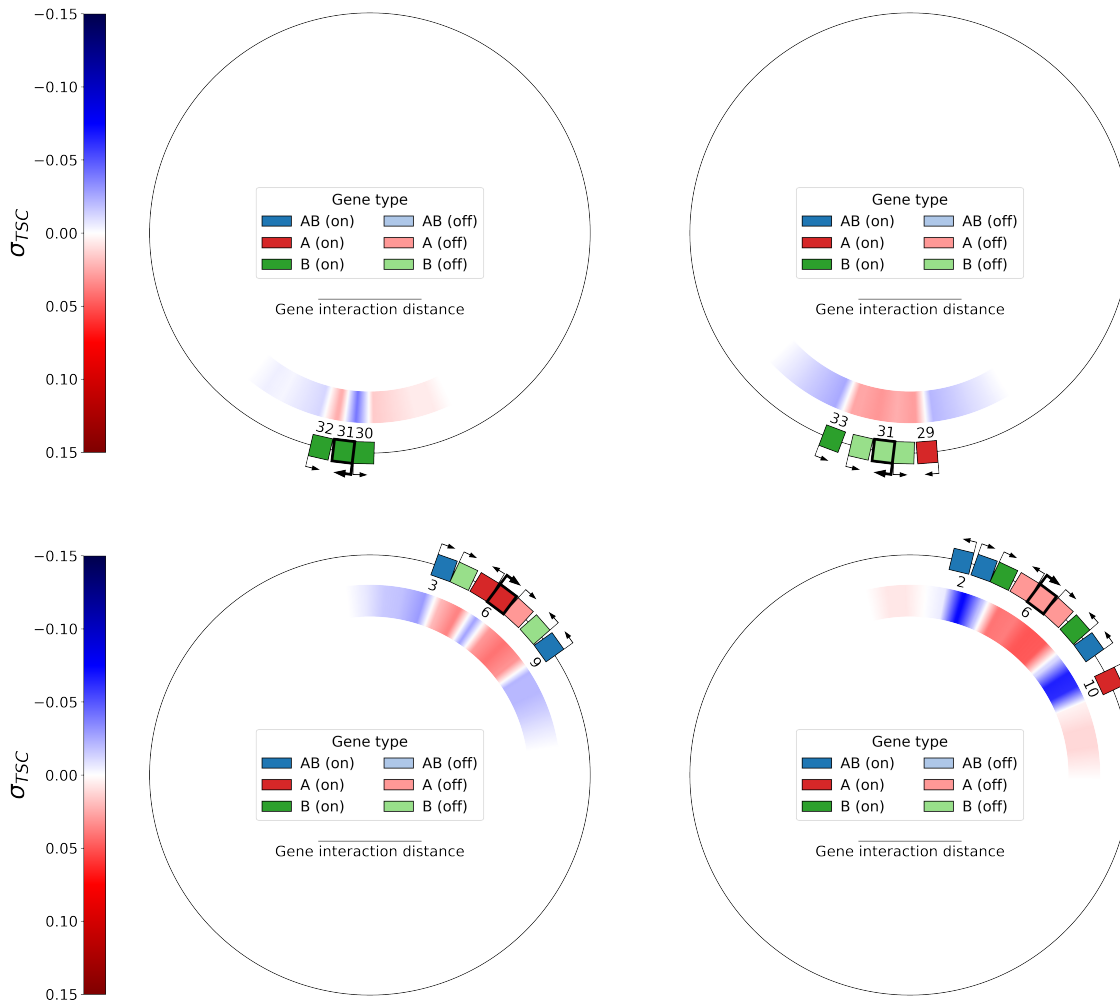


Figure 6: Top: contiguous subnetworks of size 3 (left) and 5 (right) centered around gene 31 (of type *B*, in bold) of the final best individual of replicate 21, evaluated in environment A. Bottom: contiguous subnetworks of size 7 (left) and 9 (right), centered around gene 6 (of type *A*, in bold) of the same individual, evaluated in environment B. The complete genome of this individual is shown in Figure 1.

330 Figure 6 depicts the smallest subnetworks that are required in order to obtain the inhibition of a representative gene of type *B* in environment A (top row, gene 31), and of a representative gene of type *A* in environment B (bottom row, gene 6), both taken from the genome of the same evolved individual as in Figure 1. This *B* gene is not inhibited by a subnetwork of size 3, but requires a subnetwork of size 5 in order to be inhibited, and, similarly, this *A* gene is not inhibited by a subnetwork of size 7, but requires a subnetwork of size 9 in order to be inhibited. In each case, increasing the size of the subnetwork by two (one gene on each side) drastically changes the expression level of the central

335

gene of the subnetwork, alongside with the associated level of transcription-generated supercoiling. Indeed, in the two subnetworks centered around the *B* gene (top), all 3 genes in the small subnetwork switch from activation in the small subnetwork to inhibition in the large subnetwork, and in the two  
340 subnetworks centered around the *A* gene (bottom), the two *B* genes and two out of the three central *A* genes also switch from activation to inhibition when moving from the small to the large subnetwork. In both examples, the activity of a gene does therefore not only depend only on its interaction with its closest neighbors, but with a broader section of the genome.

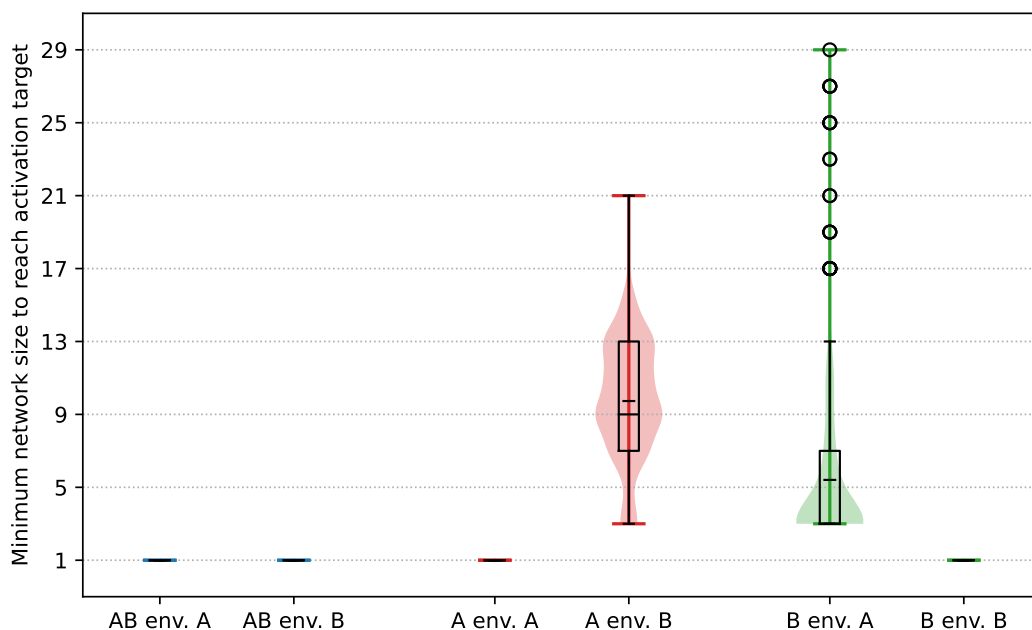


Figure 7: Minimal contiguous subnetwork size required for the central gene in the subnetwork to present the same activation state as in the complete genome, for each gene type, and in each environment. The data is computed only for genes in the best final individual of each replicate which present the correct activation state in both environments (which represents 97.7% of *AB* genes, 92.7% of *B* genes and 53.2% of *A* genes). In each case, a box plot showing quartiles and fliers is overlaid on a violin plot representing the whole distribution, and the mean is represented by the smaller tick.

We then computed these minimal subnetwork sizes for every gene that presents the correct activation state in each environment in the final best individual of each of the 30 replicates. Markedly  
345 different patterns again appear, depending on whether the targeted behavior for the gene is activation or inhibition, as depicted in Figure 7. For *AB* genes in both environments, as well as for *A* genes in environment A and *B* genes in environment B, the experimentally obtained minimum subnetwork size is 1, which is consistent with the expression profile of an isolated gene (previously shown in Figure 4).  
350 With a basal supercoiling value of  $\sigma_{basal} = -0.06$ , an isolated gene indeed experiences a high expression

level in both environments – even without interactions – in the model, as in real-world bacteria.

When the expression target of the gene is inhibition, that is for  $A$  genes in environment B and for  $B$  genes in environment A, the picture is however quite different. In this case, a significantly larger subnetwork is required in order to obtain inhibition of the focal gene: The median subnetwork size required to inhibit  $A$  genes in environment B is 9, or 4 genes on each side. For  $B$  genes, the median subnetwork size for inhibition in environment A is lower than that required for the inhibition of  $A$  genes in environment B, but higher than when the target is activation: Genes always need at least a subnetwork of size 3 (1 gene on each side), and several outliers need a subnetwork of more than 20 genes in order to obtain inhibition.

The gene regulatory networks that evolve through the transcription-supercoiling coupling therefore exhibit a structure that cannot be summarized by the pairwise interactions between neighboring genes, but that can on the contrary require the participation of a significantly larger number of genes in order to allow genes to reach their required environment-specific expression levels.

## 2.4 A Whole-Genome Gene Regulatory Network

Having shown that the transcription-supercoiling coupling plays a major role in the regulation of gene expression in our model, and that supercoiling-mediated interactions can implicate more than just neighboring genes, we then sought to describe these interactions in more detail using the framework of gene regulatory networks. The matrix of gene interactions, whose coefficients  $\frac{\partial \sigma_i}{\partial e_j}$  are the effect of the transcription of every gene on the local level of supercoiling at every other gene (and decrease linearly with distance, see Equation 1 in Methods), could seem to provide a natural graph representation of the interactions between the genes in the genome of an individual. However, as this representation does not take into account actual gene expression levels, it provides an inaccurate picture of the effective interactions between genes (for example, overestimating the influence of a weakly-expressed gene). We therefore constructed an *effective* interaction graph, by measuring the effect of gene knockouts on gene expression levels.

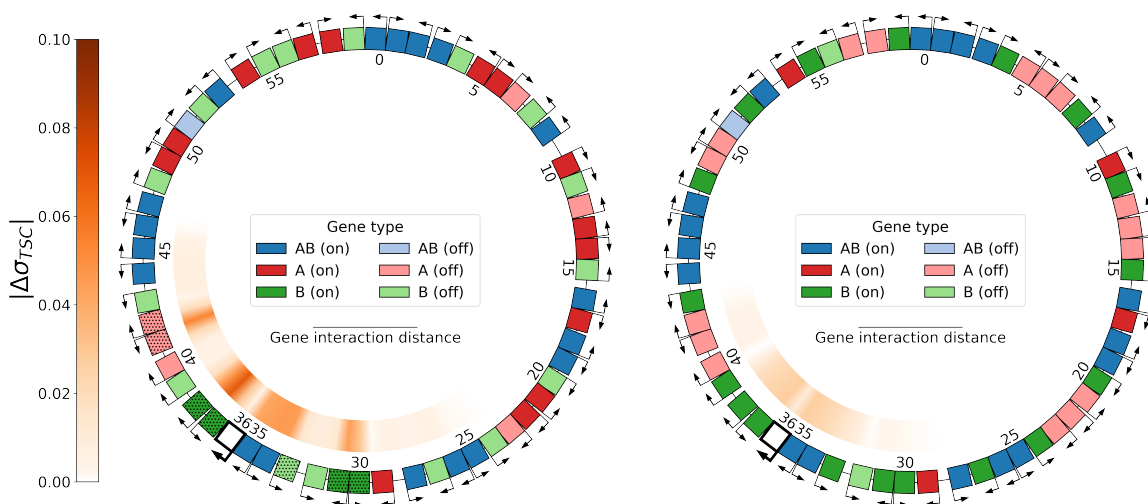


Figure 8: Knockout of gene 36 (of type *AB*, in bold, colored white) of the final best individual of replicate 21, evaluated in environments A (left) and B (right). Hatched genes represent genes whose activation state is switched by the knockout when compared to the original genome. The inner ring represents the absolute difference  $|\Delta\sigma_{TSC}|$  in the level of transcription-generated supercoiling between the knockout genome and the original genome (shown above in Figure 1).

**Gene Knockouts** Gene knockout is a genetic technique in which a gene of interest is inactivated (knocked-out) in order to study its function (in our case, its possible role as part of a gene regulatory network). In order to knock out a given gene in an individual in our model, we set the transcription rate of that gene to zero during the computation of gene expression levels (as described in Methods). This mimics a loss of function of the promoter of the gene, while keeping the intergenic distance between its upstream and downstream neighbors unchanged, thereby minimizing differences to the original individual. The result of a gene knockout on the genome of an evolved individual is shown in Figure 8. The knocked-out gene is gene 36 (bottom left of the genome), which is of type *AB* and originally activated in both environments (see Figure 1 for the original genome of the same individual). We can see that, in environment A, knocking out this gene results in a switch in the activation state of 7 genes (hatched in the left-hand side of Figure 8), and that these genes are not all contiguously located. This knockout also results in local supercoiling changes that propagate up to the bottom-left third of the genome, outside of the direct influence of the knocked-out gene. In environment B, knocking out this gene instead results in milder supercoiling changes that do not result in any gene switching state. In this example, knocking out even a single gene can therefore substantially affect gene expression levels, and lead to a switch in the activation state of other genes on the genome, even when these genes do

not directly interact with the knocked-out gene.

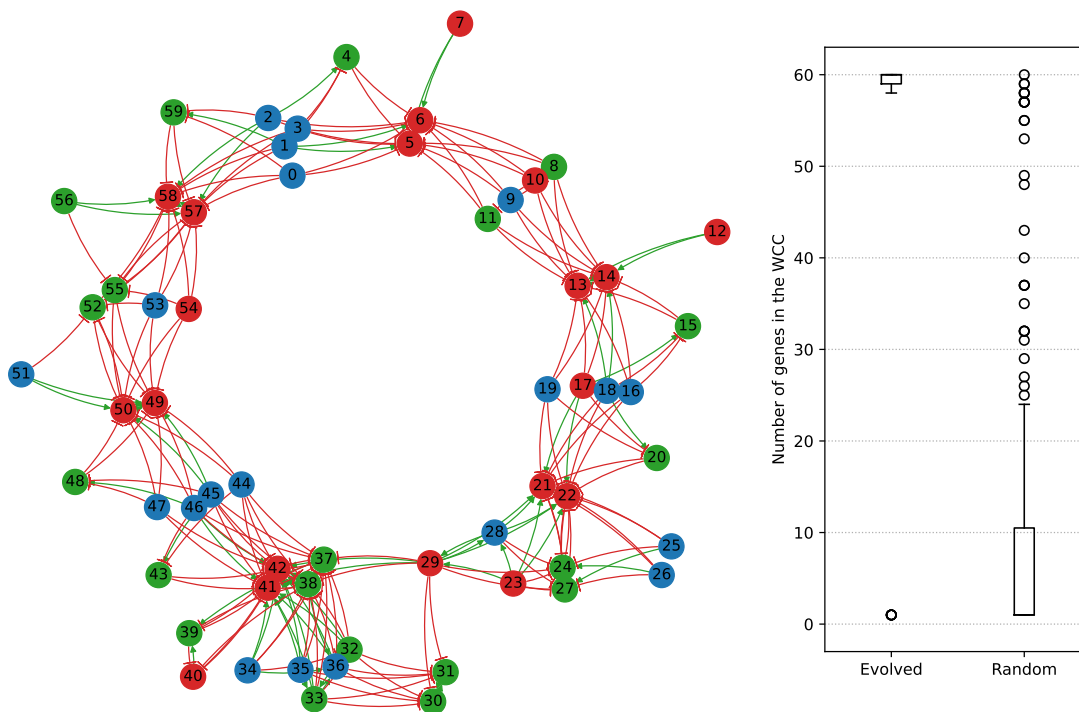


Figure 9: Left: effective interaction graph of the best individual at the last generation of replicate 21, obtained by knocking out every gene one by one and measuring the resulting gene switches in either environment. Activation edges are drawn in green, and inhibition edges in red. Gene numbering is the same as in Figures 1, 7 and 8. Right: distribution of weakly connected component (WCC) sizes in the effective interaction graphs of evolved individuals (left) compared to random individuals (right).

### Constructing the Effective Interaction Graph

We construct the effecting interaction graph in the following manner: we successively knock out every gene in the genome, and each time add edges from the knocked-out gene to every other gene whose activation state is switched by the knockout, in one environment or the other. If the knockout switches off a gene that was originally activated in the complete genome, we mark the edge as an activation edge, meaning that the knocked-out gene was necessary in order to activate the switched-off gene. If the knockout conversely switches on a gene that was originally inhibited in the complete genome, we mark the edge as an inhibition edge. If knocking out a gene switches on or off the same other gene in the two environments, we only add a single edge (even if one edge is an activation edge and the other an inhibition edge), as our main focus is on the connectedness of the resulting graph. The effective interaction graph of the example evolved

individual in Figure 8 is presented on the left-hand side of Figure 9. In this individual, there is only one weakly connected component (WCC), meaning that all the genes of this individual contribute to  
405 a single, whole-genome regulatory network.

**Structure of the Effective Interaction Graphs** In order to characterize the effective interaction graphs of evolved individuals, we compared them with the effective interaction graphs of 30 random individuals drawn using the same genome parameters (shown in Table 1 in Methods) as the initial individuals used at the beginning of evolution. The distribution of WCC sizes for each group of graphs  
410 are presented on the right-hand side of Figure 9, and they show that the effective interaction graphs of evolved individuals are clearly different from those of random individuals. Indeed, evolved genomes have WCC sizes of 58 to 60 genes (left), comprising every or nearly every gene on the genome, along with very few single-gene WCCs. In particular, in 26 out of the 30 evolved populations, the interaction graph of the best individual comprises only a single WCC that includes every gene on the genome,  
415 similarly to the interaction graph in Figure 9. In random genomes (right), on the other hand, WCC sizes span the whole range from single-gene to whole-genome WCCs, with most of the connected components counting less than 10 genes.

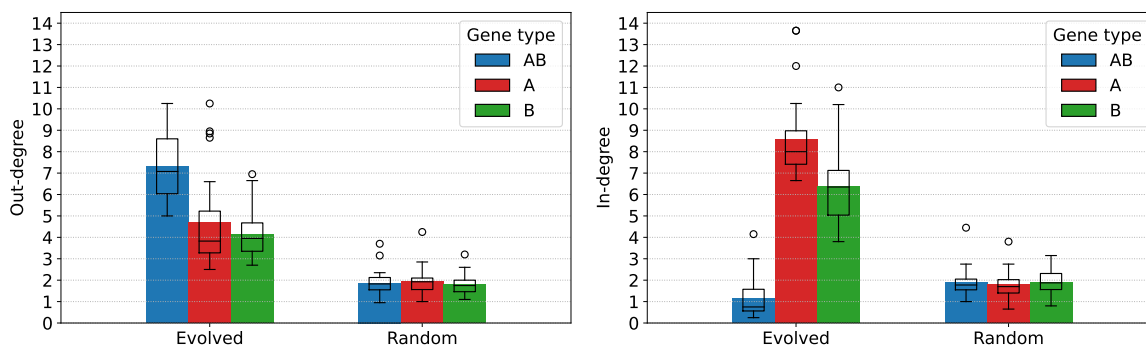


Figure 10: Left: average out-degree (number of genes switched by knocking out a given gene) of the nodes in the effective interaction graph, separated by gene type, for evolved and random individuals. Right: average in-degree (number of genes whose knockout switches a given gene) of the nodes in the effective interaction graph, separated by gene type, for evolved and random individuals.

Evolved genomes are indeed on average much more connected than random genomes, as we can see in Figure 10, which presents the out- and in-degree of genes (averaged by gene type) in the effective  
420 interaction graphs. The left-hand side of Figure 10 shows the average out-degree of each gene type (i.e., the number of genes that are switched either on or off by knocking out a gene of that type). While knocking out a gene in a random genome switches the state of a little less than 2 other genes

on average, independently of the type of the knocked-out gene, this figure is much higher in evolved genomes. Knocking out *A* or *B* genes switches 4 other genes on average, and knocking out *AB* genes switches up to 7 other genes. Through this higher connectedness, *AB* genes therefore play a quantitatively more important regulatory role than *A* genes or *B* genes. This can be explained by the fact that *AB* genes are activated – and generate more supercoiling through transcription, as shown in Figure 5 – in both environments, while most *A* and *B* genes are instead inhibited in one environment or the other.

When looking at the in-degree of genes (the number of genes whose knockout will switch a given gene on or off), we can see that evolved genomes are again much more connected on average than random genomes, and that the in-degree of genes greatly depends on their type. Indeed, *AB* genes are only switched by one other gene on average, meaning that their activation state is robust to perturbations in the regulatory network. The robustness of *AB* gene state could be expected, as these genes must have the same activation state in both environments in order to attain high fitness. On the contrary, *A* genes and *B* genes have a much higher in-degree, meaning that their activation state relies on the regulatory action of a large number of other genes. Similarly to *AB* genes, this high connectedness could be expected, as a high in-degree could make *A* and *B* genes more sensitive to the variations that these genes need to detect in order to distinguish between the two environments.

In our model, the evolution of the relative positions of genes on the genome therefore integrates local supercoiling-mediated interactions between neighboring genes into a single genome-wide regulatory network, through which all genes interact to reach their targeted expression levels.

### 3 Discussion and Perspectives

DNA supercoiling, through its effect on promoter activation and hence on gene transcription (Dorman and Dorman, 2016), is an important actor of the regulatory response of bacteria to changing environmental conditions (Martis B. et al., 2019). But gene transcription itself has long been posited to impact the level of DNA supercoiling in return, as suggested by the twin-domain model of supercoiling of Liu and Wang (1987), and it has since been shown to indeed play a major role in shaping the bacterial DNA supercoiling landscape (Visser et al., 2022), through what has been termed the transcription-supercoiling coupling (Meyer and Beslon, 2014). Taken together, these results suggest that such supercoiling-mediated interactions between the transcription rates of neighboring genes could play a part in regulating bacterial gene activity.

In this work, we therefore sought to assess the possibility of the evolution of such supercoiling-based gene regulation in an *in silico* bacteria-like model, and to determine its potential hallmarks on the local and global organization of bacterial genomes. To this end, we developed an evolutionary model of the transcription-supercoiling coupling, in which populations of individuals must evolve differentiated gene expression levels in response to different environmental conditions. We showed that, in this model, gene regulation by DNA supercoiling is indeed a sufficient mechanism to evolve environment- and gene- specific patterns of activation and inhibition. In particular, we observed the emergence of relaxation-activated genes that respond to supercoiling oppositely to the majority of genes, which are classically inhibited by DNA relaxation (Forquet et al., 2021). Our results therefore demonstrate that this response to supercoiling can result not only from promoter sequence – as in the case of the *gyrA* promoter (Menzel and Gellert, 1987) – or spacer length (Forquet et al., 2022), but also from local genome organization, as proposed by Sobetzko (2016) or El Houdaigui et al. (2019). As such, these findings suggest that supercoiling-mediated regulation could be a sufficient mechanism to fine-tune gene expression in response to environmental constraints. This regulatory role could in particular be especially important in bacteria that lack other regulatory mechanisms, such as the streamlined *B. aphidicola* (Brinza et al., 2013).

We then investigated the patterns of genome organization that underlie this transcriptional response to different supercoiling environments. At the most local scale, we found that evolved genomes in the model are enriched in divergent pairs of always-on genes that form positive feedback loops, as well as in convergent pairs that oppositely act as bistable toggle switches controlled by supercoiling rather than transcription factors (Gardner et al., 2000). The existence of such supercoiling-mediated toggle switches had been earlier posited by using mechanistic biophysical models that explicitly describe the movement of RNA polymerases during gene transcription (Sevier and Hormoz, 2022; Johnstone and Galloway, 2022), and their emergence in our model suggests that such toggle switches could indeed evolve as a means to regulate the expression of neighboring genes. Then, we showed that the local organization of the genome into convergent or divergent pairs of genes is in fact not sufficient to explain the transcriptional response of individuals to different environments, but that interactions between larger groups of neighboring genes can be required to selectively activate or inhibit genes in specific environments. Such regulation of gene expression through the interaction of groups of co-located genes could help explain the persistence of synteny segments (clusters of genes that display correlated expression levels at the supra-operonic scale) that has been evidenced in the evolutionary

histories of both *E. coli* and *S. enterica* (Junier and Rivoire, 2016). Indeed, if local interactions play  
485 a role in regulating the expression of groups of neighboring genes, genomic rearrangements that alter  
relative gene positions within these structures could disrupt their regulation and hence be evolutionarily  
unfavorable. Finally, we characterized in further detail the gene regulatory networks that evolve  
in this model by adapting the classical genetics tool of gene knockouts (Baba et al., 2006). We  
showed that supercoiling-mediated interactions integrate the entire genome of evolved individuals into  
490 a single connected regulatory network, in opposition to the sparse, disconnected networks displayed by  
randomly generated individuals. Moreover, we showed that genes play different roles in these networks  
depending on their type, corresponding to the type-specific responses to environmental variations that  
genes must display in the model. Overall, our simulations therefore demonstrate that the transcription-  
supercoiling coupling provides a strong and precise regulatory mechanism that allows for the evolution  
495 of complex regulation patterns based solely on the relative positions of genes on the genome, and can be  
sensitive to very small environmental perturbations (see Supplementary Material). They furthermore  
evidence the possible impact of this particular mode of regulation on the structure of bacterial genomes,  
both at the local and global scales.

In this work, we voluntarily kept our model as simple as possible in order to obtain easily in-  
500 terpretable results, while retaining the core concept of the transcription-supercoiling coupling. In  
particular, in order to keep simulations computationally tractable, we restricted the number of genes  
in each individual to 60, much fewer than the around 4,300 genes in the *E. coli* genome (Blattner,  
1997), but importantly keeping chromosome size much larger than the supercoiling interaction dis-  
tance, so that each gene directly interacts with a small proportion of the genome only. Increasing  
505 the number of genes of genomes in our model should in principle therefore not affect the local- and  
medium-scale patterns that we observe, nor the formation of large-scale regulatory networks, although  
such genomes might harbor several large weakly connected components rather than a single one. Sev-  
eral other relevant questions could also be studied by modifying our model appropriately. For example,  
it would be interesting to study how including transcriptional read-through, or the transcription of  
510 successive genes by a single RNA polymerase, would alter the genomic structures that evolve in our  
model. Indeed, this mechanism has also been hypothesized to play a role in the evolutionary con-  
servation of synteny segments in bacterial genomes, by correlating the expression levels of genes in  
these segments (Junier and Rivoire, 2016). Incorporating read-through in our model could therefore  
inform us about the relative importance of this mechanism compared to supercoiling-mediated reg-

515 ulation in the conservation of these genomic segments. Similarly, letting the reaction norm of gene promoters to supercoiling coevolve with genomic organization could help understand the evolution of unusual promoters such as the *gyrA* promoter, which is activated by relaxation due to its particular sequence (Menzel and Gellert, 1987). Finally, integrating a more classical model of gene regulation via transcription factors to our model, such as the one presented by Crombach and Hogeweg (2008), 520 could also help shed light on the coevolution between the different modes of gene regulation that are available to bacterial genomes. From a theoretical standpoint, a range of mechanistic biophysical models of the transcription-supercoiling coupling have been put forward, using different hypotheses in order to address related questions on this topic. Brackley et al. (2016) show a phase transition in the transcription regime as the number of RNA polymerases transcribing a given gene increases; Sevier and Hormoz (2022) show that bursty transcription can emerge from the transcription-supercoiling coupling; and Meyer and Beslon (2014) and El Houdaigui et al. (2019) try to predict gene expression levels 525 quantitatively, as a function of the local level of DNA supercoiling. An important validation of these complementary approaches would therefore be to investigate the extent to which these models, including ours, conform to one another as the level of abstraction changes. From an experimental standpoint, 530 comparing our simulated results on genome organization with data from real-world bacteria could also help determine the extent of the regulatory role of supercoiling in these organisms. One such effort would be to quantify the level of correlation between genomic organization and gene transcription levels in species with few transcription factors such as *B. aphidicola* (Brinza et al., 2013), applying the methods presented in Sobetzko (2016) to study such organisms as *E. coli* or *S. pneumoniae*. Finally, 535 from a synthetic biology point of view, a better understanding of the regulatory interactions stemming from the transcription-supercoiling coupling could help design more finely controlled artificial genetic constructs, as explored by Johnstone and Galloway (2022).

## 4 Conclusion

To the best of our knowledge, our work is the first to model the regulatory role of supercoiling on tran- 540 scription at a genomic scale, and the first to study its importance in the evolution of bacterial genomes through an evolutionary simulation approach. It demonstrates the importance of supercoiling-mediated interactions between genes on their transcription rates, and exemplifies the precision and versatility of the regulation mechanism that stems from these interactions. For experimentalists, it provides an underlying theory that could help explain the heterogeneous transcriptomic response (with both

545 up- and down-regulation of multiple genes) observed in bacteria confronted to supercoiling variations, due among others to virulence-inducing environments (Dorman, 2019) or to gyrase-inhibiting antibiotics (de la Campa et al., 2017). For evolutionists, it provides a plausible evolutionary rationale for the observed conservation of local gene order along evolutionary histories (Junier and Rivoire, 2016). Finally, for synthetic biologists, it provides a theory to help predict in finer detail the transcription  
550 levels that can be expected from a given gene syntax (Johnstone and Galloway, 2022), and thus design new forms of genetic circuits.

## 5 Methods

This section presents the model that we use throughout the manuscript to study the role of the transcription-supercoiling coupling in the evolution of gene regulation and genome organization in  
555 bacteria-like organisms. The model consists in an individual-based evolutionary simulation, in which the phenotype of every individual is computed according to a biophysical model of the effect of supercoiling on gene expression. It is based upon and refines our previous model presented in Grohens et al. (2022). We start by presenting the individual-level biophysical model, and describe how we compute gene expression levels based on their relative positions on the genome, by taking into account  
560 the interplay between DNA supercoiling and gene transcription. Then, we describe how we build an evolutionary simulation upon this individual-level model, how we evaluate the adaptation of individuals to distinct environments, and the mutational operator that we use to create new individuals and populations. Finally, we present the experimental setup that we used in order to run the simulations presented in the Results section, and discuss code and data availability.

### 5.1 Individual-Level Model of the Transcription-Supercoiling Coupling

We define the genotype of an individual as a single circular chromosome, meant to represent a bacterial chromosome. The chromosome consists in a fixed number of protein-coding genes, which are separated by non-coding intergenic segments of varying sizes, and is additionally characterized by a basal supercoiling level  $\sigma_{basal}$ . Each gene on the chromosome is characterized by its starting position  
570 (note that genes cannot overlap in our model), its orientation (on the forward or reverse strand), its length, and its basal expression level. We always consider individuals within an environment, which we define by the perturbation  $\delta\sigma_{env}$  that it imposes to the supercoiling level of the chromosome. We

define the phenotype of an individual in a given environment as the vector that holds the expression levels of all its genes. We compute this phenotype by solving the system of equations given by the interaction of the individual's genes with one another through the transcription-supercoiling coupling (described below), on a chromosome with a background supercoiling level of  $\sigma_{basal} + \delta\sigma_{env}$ .

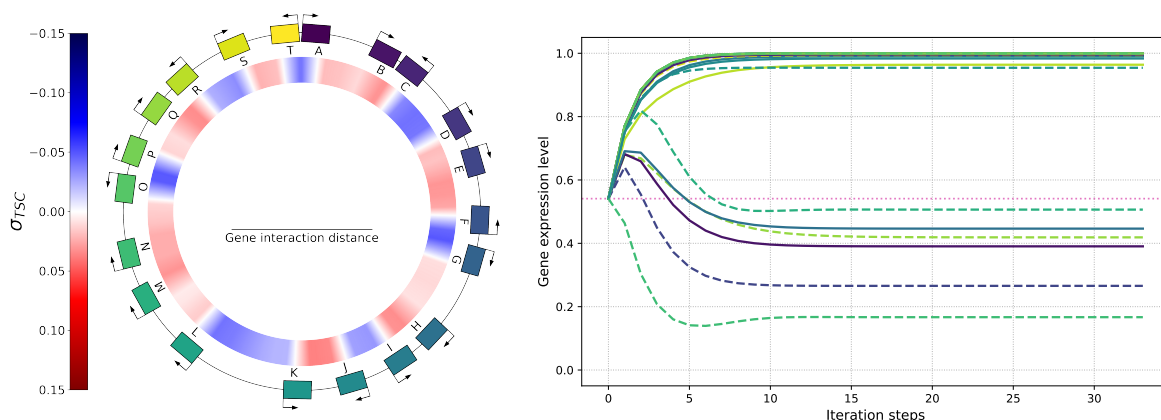


Figure 11: Left: genome (outer ring) and level of transcription-generated supercoiling ( $\sigma_{TSC}$ , inner ring) of an example individual with 20 genes placed at random positions and orientations and colored by position, with a gene length and average intergenic distance of 1 kb each, and a basal supercoiling level of  $\sigma_{basal} = -0.066$ . The individual is evaluated in an environment in which  $\delta\sigma_{env} = 0$ . Right: evolution of the expression level of each gene of the individual (reusing gene colors from the genome) during the computation of the solution to the system given by equations 2, 3, and 4, starting from initial expression levels of  $e_{1/2}$ . Solid lines represent genes on the forward strand, dashed lines genes on the reverse strand, and the dotted pink line represents  $e_{1/2}$ , the gene activation threshold.

The genome of an example individual with 20 genes is shown on the outer ring of the left-hand side panel of Figure 11. The inner ring depicts the local level along the genome of DNA supercoiling resulting from gene transcription, when this individual is evaluated in an environment with a supercoiling shift of  $\delta\sigma_{env} = 0$ . As expected from the twin-domain model of supercoiling, we can observe a buildup in negative supercoiling (in blue) between pairs of genes in divergent orientations, such as the C-D or F-G gene pairs, and a buildup in positive supercoiling (in red) between pairs of genes in convergent orientations, such as the K-J or Q-R gene pairs. The right-hand side panel of Figure 11 shows the computation of the gene expression levels for this individual in the same environment (as detailed below). Note that, in this model and throughout the manuscript, we conflate gene transcription rates with mRNA concentrations, as we assume that mRNAs are degraded at a constant rate, and as transcription rates in our model are only affected by the effect of supercoiling on transcription. We additionally conflate transcription rates with expression levels (or protein concentrations), as we again

assume proteins to be translated at a rate proportional to the associated mRNA concentrations and  
590 degraded at a constant rate.

**Effect of Transcription on Supercoiling** For an individual with a genome containing  $n$  genes, we model the influence of the transcription of each gene on the level of supercoiling at the promoter of every other gene in the form of an  $n$ -by- $n$  matrix, which we call the interaction matrix. The coefficient  $\frac{\partial \sigma_i}{\partial e_j}$  at indices  $(i, j)$  in this matrix represents the infinitesimal variation in DNA supercoiling  
595 at the promoter of gene  $i$  due to the transcription of gene  $j$ . The value of this coefficient is given by Equation 1:

$$\frac{\partial \sigma_i}{\partial e_j} = \eta \cdot c \cdot \max\left(1 - \frac{d(i, j)}{d_{max}}, 0\right) \quad (1)$$

$\eta$  gives the sign of the interaction, which depends on the position and orientation of gene  $j$  relative to gene  $i$ , according to the twin-domain model (Liu and Wang, 1987). If gene  $j$  is upstream of gene  $i$ , and if it is on the same strand as (points towards) gene  $i$ , then its transcription generates a buildup  
600 in positive supercoiling at gene  $i$  ( $\eta = 1$ ). Conversely, if gene  $j$  is upstream of gene  $i$  but on the other strand than (points away from) gene  $i$ , it generates a buildup in negative supercoiling at gene  $i$  ( $\eta = -1$ ). If gene  $j$  is instead located downstream of gene  $i$ , the sign of the interaction in each case is reversed:  $\eta = 1$  if the genes are on the same strand, and  $\eta = -1$  otherwise.

We then apply a torsional drag coefficient  $c$ , which is a high-level representation of the effect  
605 of transcription on the local supercoiling level. Finally, we model this change in supercoiling as linearly decreasing with the distance  $d(i, j)$  between genes  $i$  and  $j$ . More precisely, we consider the distance between the promoter of gene  $i$ , the position at which the local level of supercoiling affects the probability that an RNA polymerase binds to the DNA and starts transcribing gene  $i$ , and the middle of gene  $j$ , the average location of the RNA polymerases that transcribe gene  $j$ , assuming that  
610 DNA is transcribed at a constant speed. When this distance reaches a threshold of  $d_{max}$ , we consider the two genes to lie too far away to interact, and the effect vanishes. In other words,  $d_{max}$  represents the maximum gene interaction distance on either side of a gene (see Figure 11). Finally, we consider that genes do not interact with themselves, so we set  $\frac{\partial \sigma_i}{\partial e_i}$  to 0 for all  $i$ .

**Effect of Supercoiling on Transcription** In order to compute the transcription level of a given  
615 gene, we first compute the opening free energy of its promoter. This opening free energy depends on

the local supercoiling level, by following a sigmoidal curve that increases with negative supercoiling until a saturation threshold is reached (Forquet et al., 2021). In order to model this effect, we adapted the equations and parameter values presented in El Houdaigui et al. (2019), which are based on the *in vitro* analysis of the transcription of model bacterial promoters. We first compute the local level of supercoiling  $\sigma_i$  at the promoter of gene  $i$ , which is the sum of the background supercoiling level  $\sigma_{basal} + \delta\sigma_{env}$  (which is constant along the genome for any given individual in a given environment), and of the local variation in supercoiling caused by the transcription of every other gene (represented in Figure 11 as  $\sigma_{TSC}$ ):

$$\sigma_i = \sigma_{basal} + \delta\sigma_{env} + \sum_{j=1}^n \frac{\partial\sigma_i}{\partial e_j} e_j \quad (2)$$

We then compute the expression level of the gene using a thermodynamic model of transcription. First, we compute the opening free energy  $U_i$  of the promoter of gene  $i$ , which depends on  $\sigma_i$ , the level of supercoiling at the promoter and on  $\sigma_0$ , the level of supercoiling at which the opening free energy is at half its maximum level, according to the following sigmoidal function:

$$U_i = \frac{1}{1 + e^{(\sigma_i - \sigma_0)/\varepsilon}} \quad (3)$$

Finally, we compute the expression level  $e_i$  of gene  $i$  using the inverse effective thermal energy  $m$ :

$$e_i = e^{m(U_i - 1)} \quad (4)$$

The transcription level of a gene is therefore expressed in arbitrary units between  $e^{-m}$ , the minimum expression level when the promoter is most hindered by supercoiling (when  $U_i = 0$ ), and 1, the maximum expression level, when the promoter is most activated by supercoiling (when  $U_i = 1$ ). Throughout the manuscript, we describe a gene as activated if its transcription level is above the mean of these two values  $e_{1/2} = \frac{1}{2}(e^{-m} + 1)$ , and inhibited otherwise.

**Computation of Gene Expression Levels** Recall that we define the phenotype of an individual in an environment (described by  $\delta\sigma_{env}$ ) as the vector of gene expression levels that is solution to the system of equations given by Equations 2, 3 and 4, in that environment. In order to compute this phenotype, we numerically compute a solution to the system of equations by using a fixed-point iterative algorithm, starting from an initial state in which all genes are expressed at  $e_{1/2}$ . A representative example of

this computation is shown in the right-hand side panel of Figure 11. After an initially unstable phase,  
640 the algorithm quickly converges to a fixed point, which we define as the gene expression levels of that individual in that environment.

## 5.2 Evolutionary Model

Equipped with a model of the coupling between DNA supercoiling and gene transcription at the whole-genome scale, we now embed it into an evolutionary framework. In this framework, we model the  
645 evolution of a population of individuals, each behaving as described in Subsection 5.1, placed in two distinct environments named A and B. Environment A is a DNA relaxation-inducing environment, with a supercoiling shift of  $\delta\sigma_{env} = \delta\sigma_A = 0.01 > 0$ , and environment B is a DNA hypercoiling-inducing environment, with a supercoiling shift of  $\delta\sigma_{env} = \delta\sigma_B = -0.01 < 0$ . We define three types of genes by their environment-specific target expression levels:  $AB$  genes should be expressed in both  
650 environments, akin to housekeeping genes;  $A$  genes should be expressed in environment A but not in environment B; and, conversely,  $B$  genes should be expressed in environment B but not in environment A. Both latter types are meant to represent environment-specific genes, such as the pathogenic genes of *S. enterica* or *D. dadantii* (Cameron and Dorman, 2012; Hérault et al., 2014). Finally, we assign a type to each gene in the genome of each individual, ensuring that that there is the same number of  
655 genes of each type in each genome.

**Fitness** Let  $(e_A^A, e_B^A, e_{AB}^A)$  be the 3-dimensional vector representing the average gene expression level per gene type of an individual with  $n$  genes in environment A, and  $(e_A^B, e_B^B, e_{AB}^B)$  be the average gene expression per gene type of this individual in environment B. Let  $(\tilde{e}_A^A, \tilde{e}_B^A, \tilde{e}_{AB}^A)$  and  $(\tilde{e}_A^B, \tilde{e}_B^B, \tilde{e}_{AB}^B)$  be target expression values for each gene type in each environment, reflecting the gene type definitions  
660 presented above. For environment A, we choose to set  $\tilde{e}_A^A = \tilde{e}_{AB}^A = 1$ , and  $\tilde{e}_B^A = e^{-m}$ , which are respectively the maximal and minimal attainable gene expression levels in the model. Similarly, for environment B, we set  $\tilde{e}_B^B = \tilde{e}_{AB}^B = 1$ , and  $\tilde{e}_A^B = e^{-m}$ . We can then compute the sum  $g$  of the squared error (or gap) between the mean and targeted expression levels for each gene type in each environment:

$$g = \sum_{i \in \{A, B, AB\}} (e_i^A - \tilde{e}_i^A)^2 + \sum_{i \in \{A, B, AB\}} (e_i^B - \tilde{e}_i^B)^2 \quad (5)$$

Finally, we define the fitness of the individual as  $f = \exp(-k \cdot g)$ , where  $k$  is a scaling factor  
665 representing the intensity of selection: as  $k$  increases, the difference in fitness, and hence in reproductive

success, between individuals with different values of  $g$  also increases.

**Evolutionary Algorithm** We consider populations of  $N = 100$  individuals, which reproduce in non-overlapping generations. At each generation, we compute the fitness of each individual, based on its gene transcription levels in each environment (as described above). In order to create the following  
670 generation, we choose a parent at random from the current population for each individual in the new population, with a probability proportional to the fitness of the parent. Then, we create the genome of the new individual by stochastically applying mutations to the genome of its parent.

**Mutational Operator: Genomic Inversions** In order to model the evolution of genome organization, we use genomic inversions as the only mutational operator, so that genes might be reordered  
675 on the chromosome through series of inversions over evolutionary time. Note that translocations can be modeled as a series of well-chosen consecutive inversions, and are therefore implicitly present in our model. We however do not include large-scale duplications or deletions, as these rearrangements might change the number of genes; in other words, we assume gene loss or duplication to be lethal mutations in this model.

680 In order to perform a genomic inversion, we choose a start point and an end point uniformly at random in the non-coding intergenic sections of the genome. This ensures that genes cannot be broken apart by inversions (remember that we assume that gene losses are lethal). Having chosen the ends of the inversion, we extract the DNA segment between these ends and reinsert it at the same position, but in the reverse orientation. The inversion thereby reverses the orientation of every gene inside the  
685 segment, but conserves the relative positions and distances between these genes. On the contrary, the intergenic sections at the boundaries of the inversion can grow or shrink depending on the position of its start and end points, thereby allowing intergenic distances to change over evolutionary time.

Finally, when mutating an individual, we first draw the number of inversions to perform from a Poisson law of parameter  $\lambda = 2$ , meaning that the offspring of an individual will on average undergo  
690 two inversions. Then, we perform each inversion in succession as previously described, in order to obtain the final mutated offspring.

### 5.3 Experimental Setup

In order to conduct the simulations presented in the Results section, we let 30 independent populations of  $N = 100$  individuals evolve for 1,000,000 generations. We initially seeded each population with 100

695 clones of a randomly generated individual with 60 genes, or 20 genes of each type ( $A$ ,  $B$  and  $AB$ ), using a different seed for each population. For the simulations presented in the Supplementary Material, we let 15 additional independent populations evolve for 250,000 generations, for each set of environmental perturbation values ( $\sigma_A = 0.001$  and  $\sigma_B = -0.001$ , and  $\sigma_A = 0.0001$  and  $\sigma_B = -0.0001$  respectively).

The parameter values that we used are given in Table 1, and can be broadly grouped into genome-  
700 level parameters (gene length, intergenic distance, basal supercoiling level and supercoiling transmission distance) and promoter-level parameters (promoter opening threshold and effective thermal energy, crossover width). Both the genome-level parameters that describe the chromosome and the promoter-level parameters used to compute the transcriptional response to supercoiling were taken from experimental values measured in *E. coli*. Note that, in our model, we introduce the torsional  
705 drag coefficient  $c$  as a new parameter that represents the influence of torsional drag on the local level of supercoiling. We empirically chose its value so that this effect is of the same magnitude as that of the other sources of supercoiling variations (i.e., environmental perturbations) in the model.

Parameter	Symbol	Value	Reference
Gene length	$l$	1,000 bp	Blattner (1997)
Initial intergenic distance	$d_0$	125 bp	Blattner (1997)
Supercoiling transmission distance	$d_{max}$	5,000 bp	Postow et al. (2004)
Basal supercoiling level	$\sigma_{basal}$	-0.066	Crozat et al. (2005)
Torsional drag coefficient	$c$	0.03	
Promoter opening threshold	$\sigma_{opt}$	-0.042	El Houdaigui et al. (2019)
Inverse effective thermal energy	$m$	2.5	El Houdaigui et al. (2019)
Crossover width	$\varepsilon$	0.005	El Houdaigui et al. (2019)

Table 1: Parameter values of the transcription-supercoiling coupling model used in the evolutionary simulations. The upper set of parameters is the genome-level parameters, the lower set the promoter-level parameters, both taken from the *E. coli* literature; the middle parameter is a new addition from our model.

## 5.4 Reproducibility and data availability

We implemented the simulation in Python, and optimized the computationally heavy parts using the  
710 `numba` package (Lam et al., 2015). The source code for the simulation, as well as the notebooks used for data analysis, are available online at the following address: <https://gitlab.inria.fr/tgrohens/evotsc>. Running the complete set of simulations took around 36 hours of computation on a server using a 24-core Intel Xeon E5-2620 v3 @ 2.40GHz CPU, with each replicate running on a single core and using approximately 300 MB of RAM. The data from the main run of the

715 experiment is available online on the Zenodo platform, at the following address: <https://doi.org/10.5281/zenodo.7062757>. The supplementary data is available at the following address: <https://doi.org/10.5281/zenodo.7789492>.

## References

- Baba, T., Ara, T., Hasegawa, M., Takai, Y., Okumura, Y., Baba, M., Datsenko, K. A., Tomita, M.,  
720 Wanner, B. L., and Mori, H. (2006). “Construction of *Escherichia Coli* K-12 In-frame, Single-gene Knockout Mutants: The Keio Collection”. *Molecular Systems Biology* 2.1. DOI: 10.1038/msb4100050.
- Blattner, F. R. (1997). “The Complete Genome Sequence of *Escherichia Coli* K-12”. *Science* 277.5331, pp. 1453–1462. DOI: 10.1126/science.277.5331.1453.
- 725 Brackley, C. A., Johnson, J., Bentivoglio, A., Corless, S., Gilbert, N., Gonnella, G., and Marenduzzo, D. (2016). “Stochastic Model of Supercoiling-Dependent Transcription”. *Physical Review Letters* 117.1, p. 018101. DOI: 10.1103/PhysRevLett.117.018101.
- Brinza, L., Calevro, F., and Charles, H. (2013). “Genomic Analysis of the Regulatory Elements and Links with Intrinsic DNA Structural Properties in the Shrunken Genome of *Buchnera*”. *BMC*  
730 *Genomics* 14.1, p. 73. DOI: 10.1186/1471-2164-14-73.
- Cameron, A. D. S. and Dorman, C. J. (2012). “A Fundamental Regulatory Mechanism Operating through OmpR and DNA Topology Controls Expression of *Salmonella* Pathogenicity Islands SPI-1 and SPI-2”. *PLoS Genetics* 8.3, e1002615. DOI: 10.1371/journal.pgen.1002615.
- Champoux, J. J. (2001). “DNA Topoisomerases: Structure, Function, and Mechanism”. *Annual Review*  
735 *of Biochemistry* 70.1, pp. 369–413. DOI: 10.1146/annurev.biochem.70.1.369.
- Crombach, A. and Hogeweg, P. (2008). “Evolution of Evolvability in Gene Regulatory Networks”. *PLoS Computational Biology* 4.7, e1000112. DOI: 10.1371/journal.pcbi.1000112.
- Crozat, E., Winkworth, C., Gaffe, J., Hallin, P. F., Riley, M. A., Lenski, R. E., and Schneider, D. (2010). “Parallel Genetic and Phenotypic Evolution of DNA Superhelicity in Experimental Populations of  
740 *Escherichia Coli*”. *Molecular Biology and Evolution* 27.9, pp. 2113–2128. DOI: 10.1093/molbev/msq099.
- Crozat, E., Philippe, N., Lenski, R. E., Geiselmann, J., and Schneider, D. (2005). “Long-Term Experimental Evolution in *Escherichia Coli*. XII. DNA Topology as a Key Target of Selection”. *Genetics* 169.2, pp. 523–532. DOI: 10.1534/genetics.104.035717.

- 745 de la Campa, A. G., Ferrándiz, M. J., Martín-Galiano, A. J., García, M. T., and Tirado-Vélez, J. M. (2017). “The Transcriptome of *Streptococcus Pneumoniae* Induced by Local and Global Changes in Supercoiling”. *Frontiers in Microbiology* 8, p. 1447. DOI: 10.3389/fmicb.2017.01447.
- Dorman, C. J. (2019). “DNA Supercoiling and Transcription in Bacteria: A Two-Way Street”. *BMC Molecular and Cell Biology* 20.1, p. 26. DOI: 10.1186/s12860-019-0211-6.
- 750 Dorman, C. J. and Dorman, M. J. (2016). “DNA Supercoiling Is a Fundamental Regulatory Principle in the Control of Bacterial Gene Expression”. *Biophysical Reviews* 8.3, pp. 209–220. DOI: 10.1007/s12551-016-0205-y.
- El Hanafi, D. and Bossi, L. (2000). “Activation and Silencing of Leu-500 Promoter by Transcription-Induced DNA Supercoiling in the *Salmonella* Chromosome: Transcription-dependent Modulation
- 755 of Leu-500 Promoter in topA Mutants”. *Molecular Microbiology* 37.3, pp. 583–594. DOI: 10.1046/j.1365-2958.2000.02015.x.
- El Houdaigui, B., Forquet, R., Hindré, T., Schneider, D., Nasser, W., Reverchon, S., and Meyer, S. (2019). “Bacterial Genome Architecture Shapes Global Transcriptional Regulation by DNA Supercoiling”. *Nucleic Acids Research* 47.11, pp. 5648–5657. DOI: 10.1093/nar/gkz300.
- 760 Ferrandiz, M.-J., Martin-Galiano, A. J., Schwartzman, J. B., and de la Campa, A. G. (2010). “The Genome of *Streptococcus Pneumoniae* Is Organized in Topology-Reacting Gene Clusters”. *Nucleic Acids Research* 38.11, pp. 3570–3581. DOI: 10.1093/nar/gkq106.
- Forquet, R., Nasser, W., Reverchon, S., and Meyer, S. (2022). “Quantitative Contribution of the Spacer Length in the Supercoiling-Sensitivity of Bacterial Promoters”. *Nucleic Acids Research*
- 765 50.13, pp. 7287–7297. DOI: 10.1093/nar/gkac579.
- Forquet, R., Pineau, M., Nasser, W., Reverchon, S., and Meyer, S. (2021). “Role of the Discriminator Sequence in the Supercoiling Sensitivity of Bacterial Promoters”. *mSystems* 6.4. DOI: 10.1128/mSystems.00978-21.
- Gardner, T. S., Cantor, C. R., and Collins, J. J. (2000). “Construction of a Genetic Toggle Switch in
- 770 *Escherichia Coli*”. *Nature* 403.6767, pp. 339–342. DOI: 10.1038/35002131.
- Grohens, T., Meyer, S., and Beslon, G. (2022). “A Genome-Wide Evolutionary Simulation of the Transcription-Supercoiling Coupling”. *Artificial Life* 28.4, pp. 440–457. DOI: 10.1162/artl\_a\_00373.

- Guo, M. S., Kawamura, R., Littlehale, M. L., Marko, J. F., and Laub, M. T. (2021). “High-Resolution,  
775 Genome-Wide Mapping of Positive Supercoiling in Chromosomes”. *eLife* 10, e67236. DOI: 10.7554/  
eLife.67236.
- Hérault, E., Reverchon, S., and Nasser, W. (2014). “Role of the LysR-type Transcriptional Regulator  
PecT and DNA Supercoiling in the Thermoregulation of *Pel* Genes, the Major Virulence Factors  
in *Dickeya Dadantii*: *Dickeya Dadantii* PecT Protein and Virulence Thermoregulation”. *Environ-*  
780 *mental Microbiology* 16.3, pp. 734–745. DOI: 10.1111/1462-2920.12198.
- Hsieh, L. S., Rouviere-Yaniv, J., and Drlica, K. (1991). “Bacterial DNA Supercoiling and [ATP]/[ADP]  
Ratio: Changes Associated with Salt Shock.” *Journal of Bacteriology* 173.12, pp. 3914–3917. DOI:  
10.1128/JB.173.12.3914-3917.1991.
- Johnstone, C. P. and Galloway, K. E. (2022). “Supercoiling-Mediated Feedback Rapidly Couples and  
785 Tunes Transcription”. *Cell Reports* 41.3, p. 111492. DOI: 10.1016/j.celrep.2022.111492.
- Junier, I. and Rivoire, O. (2016). “Conserved Units of Co-Expression in Bacterial Genomes: An Evo-  
lutionary Insight into Transcriptional Regulation”. *PLoS ONE* 11.5, e0155740. DOI: 10.1371/  
journal.pone.0155740.
- Krogh, T. J., Møller-Jensen, J., and Kaleta, C. (2018). “Impact of Chromosomal Architecture on  
790 the Function and Evolution of Bacterial Genomes”. *Frontiers in Microbiology* 9, p. 2019. DOI:  
10.3389/fmicb.2018.02019.
- Lam, S. K., Pitrou, A., and Seibert, S. (2015). “Numba: A LLVM-based Python JIT Compiler”.  
*Proceedings of the Second Workshop on the LLVM Compiler Infrastructure in HPC - LLVM '15*.  
Austin, Texas: ACM Press, pp. 1–6. DOI: 10.1145/2833157.2833162.
- 795 Lenski, R. E. (2023). “Revisiting the Design of the Long-Term Evolution Experiment with *Escherichia*  
*Coli*”. *Journal of Molecular Evolution*. DOI: 10.1007/s00239-023-10095-3.
- Lenski, R. E., Rose, M. R., Simpson, S. C., and Tadler, S. C. (1991). “Long-Term Experimental Evolu-  
tion in *Escherichia Coli*. I. Adaptation and Divergence During 2,000 Generations”. *The American*  
*Naturalist* 138.6, pp. 1315–1341. JSTOR: 2462549.
- 800 Liu, L. F. and Wang, J. C. (1987). “Supercoiling of the DNA Template during Transcription.” *Proceed-*  
*ings of the National Academy of Sciences* 84.20, pp. 7024–7027. DOI: 10.1073/pnas.84.20.7024.
- Marshall, D. G., Bowe, F., Hale, C., Dougan, G., and Dorman, C. J. (2000). “DNA Topology and  
Adaptation of *Salmonella Typhimurium* to an Intracellular Environment”. *Phil. Trans. R. Soc.*  
*Lond. B* 355, pp. 565–574. DOI: 10.1098/rstb.2000.0598.

- 805 Martis B., S., Forquet, R., Reverchon, S., Nasser, W., and Meyer, S. (2019). “DNA Supercoiling: An Ancestral Regulator of Gene Expression in Pathogenic Bacteria?” *Computational and Structural Biotechnology Journal* 17, pp. 1047–1055. DOI: 10.1016/j.csbj.2019.07.013.
- Menzel, R. and Gellert, M. (1987). “Modulation of Transcription by DNA Supercoiling: A Deletion Analysis of the Escherichia Coli gyrA and gyrB Promoters.” *Proceedings of the National Academy of Sciences* 84.12, pp. 4185–4189. DOI: 10.1073/pnas.84.12.4185.
- 810 Meyer, S. and Beslon, G. (2014). “Torsion-Mediated Interaction between Adjacent Genes”. *PLoS Computational Biology* 10.9, e1003785. DOI: 10.1371/journal.pcbi.1003785.
- Muskhelishvili, G., Forquet, R., Reverchon, S., Meyer, S., and Nasser, W. (2019). “Coherent Domains of Transcription Coordinate Gene Expression During Bacterial Growth and Adaptation”. *Microorganisms* 7.12, p. 694. DOI: 10.3390/microorganisms7120694.
- 815 Peter, B. J., Arsuaga, J., Breier, A. M., Khodursky, A. B., Brown, P. O., and Cozzarelli, N. R. (2004). “Genomic Transcriptional Response to Loss of Chromosomal Supercoiling in Escherichia Coli”. *Genome Biology* 5, R87. DOI: 10.1186/gb-2004-5-11-r87.
- Pineau, M., Martis B., S., Forquet, R., Baude, J., Villard, C., Grand, L., Popowycz, F., Soulère, L., Hommais, F., Nasser, W., Reverchon, S., and Meyer, S. (2022). “What Is a Supercoiling-Sensitive Gene? Insights from Topoisomerase I Inhibition in the Gram-negative Bacterium *Dickeya Dadantii*”. *Nucleic Acids Research* 50.16, pp. 9149–9161. DOI: 10.1093/nar/gkac679.
- 820 Postow, L., Hardy, C. D., Arsuaga, J., and Cozzarelli, N. R. (2004). “Topological Domain Structure of the Escherichia Coli Chromosome”. *Genes & Development* 18.14, pp. 1766–1779. DOI: 10.1101/gad.1207504.
- 825 Rhee, K. Y., Opel, M., Ito, E., Hung, S.-p., Arfin, S. M., and Hatfield, G. W. (1999). “Transcriptional Coupling between the Divergent Promoters of a Prototypic LysR-type Regulatory System, the ilvYC Operon of Escherichia Coli”. *Proceedings of the National Academy of Sciences* 96.25, pp. 14294–14299. DOI: 10.1073/pnas.96.25.14294.
- 830 Sevier, S. A. and Hormoz, S. (2022). “Collective Polymerase Dynamics Emerge from DNA Supercoiling during Transcription”. *Biophysical Journal* 121.21, pp. 4153–4165. DOI: 10.1016/j.bpj.2022.09.026.
- Sobetzko, P. (2016). “Transcription-Coupled DNA Supercoiling Dictates the Chromosomal Arrangement of Bacterial Genes”. *Nucleic Acids Research* 44.4, pp. 1514–1524. DOI: 10.1093/nar/gkw007.

- 835 Sutormin, D., Galivondzhyan, A., Musharova, O., Travin, D., Rusanova, A., Obraztsova, K., Borukhov, S., and Severinov, K. (2022). “Interaction between Transcribing RNA Polymerase and Topoisomerase I Prevents R-loop Formation in *E. Coli*”. *Nature Communications* 13.1, p. 4524. DOI: 10.1038/s41467-022-32106-5.
- Tobe, T., Yoshikawa, M., and Sasakawa, C. (1995). “Thermoregulation of *virB* Transcription in *Shigella Flexneri* by Sensing of Changes in Local DNA Superhelicity”. *Journal of Bacteriology* 177.4, pp. 1094–1097. DOI: 10.1128/jb.177.4.1094-1097.1995.
- 840 Travers, A. and Muskhelishvili, G. (2005). “DNA Supercoiling — a Global Transcriptional Regulator for Enterobacterial Growth?” *Nature Reviews Microbiology* 3.2, pp. 157–169. DOI: 10.1038/nrmicro1088.
- Visser, B. J., Sharma, S., Chen, P. J., McMullin, A. B., Bates, M. L., and Bates, D. (2022). “Pso-  
845 ralen Mapping Reveals a Bacterial Genome Supercoiling Landscape Dominated by Transcription”. *Nucleic Acids Research* 50.8, pp. 4436–4449. DOI: 10.1093/nar/gkac244.
- Webber, M. A., Ricci, V., Whitehead, R., Patel, M., Fookes, M., Ivens, A., and Piddock, L. J. V. (2013). “Clinically Relevant Mutant DNA Gyrase Alters Supercoiling, Changes the Transcriptome,  
850 and Confers Multidrug Resistance”. *mBio* 4.4. DOI: 10.1128/mBio.00273-13.